

Time-lagged impact of spring sensible heat over the Tibetan Plateau on the summer rainfall anomaly in East China: case studies using the WRF model

Ziqian Wang · Anmin Duan · Guoxiong Wu

Received: 19 January 2013 / Accepted: 6 May 2013 / Published online: 21 May 2013
© Springer-Verlag Berlin Heidelberg 2013

Abstract This study explores the time-lagged impact of the spring sensible heat (SH) source over the Tibetan Plateau (TP) on the summer rainfall anomaly in East China using the Weather Research and Forecasting model. Numerical experiments for 2003 indicate that a spring SH anomaly over the TP can maintain its impact until summer and lead to a strong atmospheric heat source, characterized both by the enhanced SH over the western TP and enhanced latent heat of condensation to the east. Wave activity diagnosis reveals that the enhanced TP heating forces a Rossby wave train over the downstream regions. A cyclonic response over the northeast TP brings about a low-level northerly anomaly over northern China, while an anticyclonic response over the western Pacific enhances the subtropical high and the low-level southerly on its western flank. As a result, cold and dry airflow from mid-high latitudes, and warm and wet airflow from tropical oceans converge around the Huaihe River basin. In addition, warm advection originating from the TP induces vigorous ascending motion over the convergence belt. Under these favorable circulation conditions the eastward-propagating vortexes initiated over the TP intensify the torrential rainfall processes over the Huaihe River basin. In contrast, additional experiments considering the year 2001 with weak spring SH over the TP and an overall southward

retreat of the summer rainfall belt in East China further demonstrate the role of spring SH over the TP in regulating the interannual variability of EASM in terms of wave activity and synoptic disturbances.

Keywords Spring sensible heat (SH) · Tibetan Plateau (TP) · East Asian summer monsoon (EASM) · Summer rainfall

1 Introduction

The impact of thermal forcing over the Tibetan Plateau (TP) on the East Asian summer monsoon (EASM) and corresponding precipitation patterns has been widely investigated. Results based on both data analysis and numerical simulation have revealed that the diabatic heating over the TP facilitates an early monsoon onset and a strong EASM circulation, which corresponds to a more northward extent of the rainfall belt over East China (e.g., Ye and Gao 1979; Wu et al. 1997; Zhao and Chen 2001; Duan and Wu 2005; Wang et al. 2008; Duan et al. 2012; Liu et al. 2012).

Before the rainy season, the thermal conditions over the TP are represented by the snow cover/depth in winter-spring or the sensible heat (SH) source in spring. An increase in snow cover/depth can delay the monsoon onset and noticeably weaken the intensity of the EASM, resulting in a decrease in precipitation in southern China and an increase in the Yangtze and Huaihe River basins (e.g., Qian et al. 2003; Zhang et al. 2004b; Zhao et al. 2007). However, a recent study by Wu and Kirtman (2007) argued that in most regions of Eurasia, snow depth anomalies can persist from winter to spring whereas snow cover anomalies cannot, and that spring snow cover over the TP has a

Z. Wang · A. Duan (✉) · G. Wu
State Key Laboratory of Numerical Modelling for Atmospheric Sciences and Geophysical Fluid Dynamics (LASG), Institute of Atmospheric Physics (IAP), Chinese Academy of Sciences (CAS), P. O. Box 9804, Beijing 100029, China
e-mail: amduan@lasg.iap.ac.cn

Z. Wang
University of Chinese Academy of Sciences,
Beijing 100049, China

moderate positive correlation only with spring rainfall in southern China. Moreover, this correlation may include the effects of El Niño-Southern Oscillation (ENSO). It might be related to the fact that snow cover/depth is far from widespread over the TP, with appreciable snow cover only in the peripheral mountains. In the vast interior, snow cover is rare or very thin, patchy, and of short duration (Wu and Qian 2003; Qin et al. 2006). The complicated interactions of snow cover/depth, soil moisture, frozen soil, albedo, and surface heat flux mean that the physical mechanisms linking winter-spring snow and the EASM are far from clear (Yanai and Wu 2006; Gao et al. 2011).

In spring, the air column over the TP changes from a heat sink to a source due to the rapidly enhanced SH (e.g., Ye and Gao 1979; Luo and Yanai 1983, 1984; Luo and Chen 1995; Wu et al. 1997). A robust statistical relationship between the spring SH source over the TP and summer rainfall pattern in East China has been well documented; i.e., strong spring SH over the TP usually corresponds to above normal rainfall in the Yangtze and Huaihe River basins (e.g., Luo and Chen 1995; Zhao and Chen 2001; Duan et al. 2005).

Most studies of the impact of the winter-spring thermal condition over the TP on the EASM have focused on the timing of the monsoon onset, the intensity of monsoon circulation systems, and the rainfall anomaly with emphasis on the large-scale land-sea thermal contrast, whereas its impact on the intraseasonal and synoptic-scale variability of the EASM has received less attention. Many synoptic systems in East China have their origin over the TP, and such eastward-moving systems usually cause extremely heavy rain and severe storms (Tao and Ding 1981). A notable case is the devastating flood in the Yangtze River basin of 1998, when convective activity over the TP contributed to the heavy rain (Yasunari and Miwa 2006). Early studies recognized that the genesis and development of TP synoptic systems are greatly influenced by surface thermal conditions. For example, using the Geophysical Fluid Dynamics Laboratory (GFDL) limited-area mesoscale simulation model, Wang (1987) found that surface SH can enhance disturbances in the TP boundary layer through a dramatic reduction in static stability. Li et al. (2002) showed that the surface SH plays an important role in the formation and intensification of a vortex over the TP, but only when the center of the vortex matches up with the surface heating field.

How does the spring SH anomaly over the TP retain its influence until summer and affect the local atmospheric heat source? Why does the strong spring SH source over the TP favor excessive precipitation in the Yangtze and Huaihe River basins? This work seeks to answer these questions by numerical simulation using the regional Weather Research and Forecasting (WRF) model for two

cases in 2003 and 2001, which have different spring SH conditions over the TP and summer rainfall patterns in East China. The remainder of this manuscript is organized as follows. In Sect. 2 the dataset and experimental design are briefly described. Section 3 presents both the data analysis and the control run results for 2003. Section 4 discusses the possible mechanism by which the SH anomaly over the TP contributes to torrential precipitation and flooding over the Huaihe River valley, and discusses the 2001 case study. Finally, an overall summary and discussion are presented in Sect. 5.

2 Data and experimental design

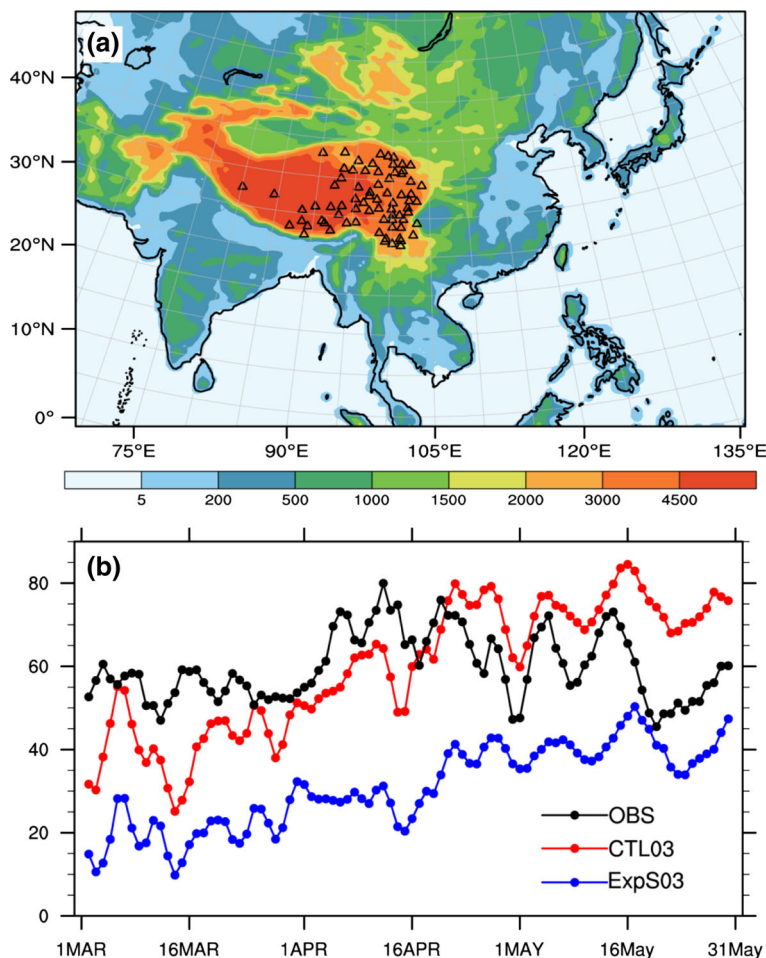
2.1 Data

The data employed in this study include historical 6-hourly observations of land surface temperature, air temperature at 2 m above the land surface, and 10 m wind speed at 73 stations over the central and eastern TP (shown in Fig. 1a) from 1980 to 2008. SH was calculated by the bulk aerodynamic method (for details see Duan et al. 2011). Daily precipitation records from 602 stations in China during the same period were provided by the China Meteorological Administration (CMA). We also used Tropical Rainfall Measuring Mission (TRMM) 3B42 daily rainfall data (Huffman et al. 2007), with $0.25^\circ \times 0.25^\circ$ horizontal resolution. The atmospheric circulation dataset is derived from the National Centers for Environmental Prediction final analysis data (NCEP-FNL, <http://rda.ucar.edu/datasets/ds083.2/>) with a 6-h interval and $1^\circ \times 1^\circ$ horizontal resolution. The daily Optimum Interpolated Sea Surface Temperature (OISST, Reynolds et al. 2007) on a $0.25^\circ \times 0.25^\circ$ grid was used to drive the WRF.

2.2 Experimental design

The model used in this study is the non-hydrostatic Advanced Research WRF model (version 3.4), which has previously been employed to simulate variations in the EASM (e.g., Kim and Hong 2010; Kim and Wang 2011; Yang et al. 2011). Physical packages include the Lin cloud microphysics scheme (Lin et al. 1983), the Grell-Devenyi (GD) convective scheme (Grell and Devenyi 2002), the NOAA land-surface model (Chen and Dudhia 2001), the BouLac planetary boundary layer (PBL) scheme (Bougeault and Lacarrère 1989), a Goddard shortwave scheme (Chou and Suarez 1999), and the Rapid Radiative Transfer Model (RRTM) for longwave radiation (Mlawer et al. 1997). The simulation domain covers most parts of Asia and adjacent oceans with 181 grid points along the east-west direction and 131 along the north-south direction (the

Fig. 1 **a** WRF model domain and terrain height (*shading*, m). **b** Temporal evolution of the spring (March–May) observed daily sensible heat (SH) averaged from 73 stations (*Triangles in (a)*) over the TP (*black*) and the corresponding simulated results in the CTL03 (*red*) and ExpS03 (*blue*) runs, in units of W m^{-2}



buffer zone has 10 grid points). A Lambert projection is adopted and the domain is centered at 30°N , 102.5°E (Fig. 1a). The model has a 45-km horizontal resolution and 35 vertical layers with a terrain-following sigma coordinate and a prescribed model top at 50 hPa. The initial state of the atmosphere and lateral boundary conditions (updated every 6 h) are from NCEP-FNL, and the sea surface temperature (SST) forcing dataset is OISST, updated daily.

Two ensemble experiments for the 2003 case study (Table 1) were performed under different SH conditions over the TP during spring (0000UTC March 1–1800UTC May 31). Results from the control experiment (CTL03), in which spring SH intensity over the TP is maintained at 100 %, are used to test WRF performance in simulating the 2003 EASM. To illustrate the contribution of the spring SH anomaly over the TP, we carried out a sensitivity experiment (ExpS03), in which the intensity of spring SH at grid cells where terrain is higher than 2000 m over the main TP area (Fig. 1a; $25\text{--}40^{\circ}\text{N}$, $70\text{--}105^{\circ}\text{E}$) is specified to be 50 % of the normal. In detail, it is achieved by setting the spring surface SH released into the atmosphere to be 50 % at each modeling time step and each grid over the select region, while the land surface energy balance is kept unchanged

(meaning the SH is still computed by the land model at each time step and allowed to impact land surface temperature). This method is exactly the same as Wu et al. (2012). Except for the modified spring SH, other settings in ExpS03 are the same as in CTL03. Each of the ensemble experiments has five members with different initial conditions at 0000UTC, 0600UTC, 1200UTC and 1800UTC February 28, and 0000UTC March 1, respectively, and each simulation ends at 1800UTC August 31 2003. Figure 1b shows the evolution of daily SH averaged over 73 stations from the two experiments and from observations: the spring SH in the CTL03 run is comparable with the observations.

To confirm the conclusions from the 2003 case study, we designed two similar ensemble experiments for 2001 where the heating conditions are reversed (Table 1). The spring SH intensity over the TP in the control experiment (CTL01) is maintained at 100 %, while it is specified to be 150 % of the normal in the sensitivity experiment (ExpS01). Again, each of the ensemble experiments has five members with different initial conditions at 0000UTC, 0600UTC, 1200UTC and 1800UTC February 28, and 0000UTC March 1 2001 respectively, and each simulation

Table 1 Experimental design

Experiments	Spring SH intensity over the TP	Goal
CTL03	100 %	Examine the WRF performance of 2003 EASM
ExpS03	50 % of the normal	Estimate effects of spring SH anomaly over the TP on 2003 EASM
CTL01	100 %	Examine the WRF performance of 2001 EASM
ExpS01	150 % of the normal	Estimate effects of spring SH anomaly over the TP on 2001 EASM

ends at 1800UTC August 31 2001. The other experimental settings of physical schemes and model domain in 2001 are the same as for 2003.

Besides the thermal forcing over the TP, ENSO also contributes to the variability of the EASM (Fu and Teng 1988; Wang et al. 2000; Wu et al. 2009). To highlight the effect of spring SH over the TP, we choose years without a strong ENSO event. In the winter preceding 2001 there is no strong ENSO event, while for the 2003 case, a moderate El Niño occurs in the preceding winter but is damped quickly in spring (figure not shown). Anomalously low snowfall occurred over the TP during the winter-spring of 2000–2001 (Ai 2002) and 2002–2003 (Yang et al. 2004). Therefore, the selection of these case studies excludes the apparent influence on the EASM of heavy snow cover/depth.

3 Observations and the control run for 2003

3.1 Observations

Figure 2a shows the standardized anomalies of the 73-station-averaged spring SH with linear trend excluded over the central-eastern TP for 1980–2008. In 2003 (2001) the spring SH over the TP is obviously stronger (weaker) than normal with the anomaly exceeding one standard deviation. The correlation field between the 73-station-averaged spring SH index over the TP and the summer (June–August, JJA) precipitation at 602 stations over China during 1980–2008 is displayed in Fig. 2b. It suggests that when the spring SH over the TP is above normal, a significant positive precipitation anomaly appears in the mid and lower reaches of the Yangtze River and the Huaihe River basin but a significant negative precipitation anomaly occurs over South China. This relationship is also seen in the composite analysis shown in Fig. 2c, in which the summer precipitation difference field is derived from the four strongest spring SH years over the TP (1987, 1991, 1995, 2003) and the four weakest years (1981, 1997, 2001, 2005).

Above-normal precipitation and flooding occurred over the Huaihe valley in 2003, which was a strong EASM year. This was the worst flood disaster along the Huaihe River since 1991 (Zhang et al. 2004a). Meanwhile, most parts of

South China suffered high temperatures (figure not shown) and dry weather (Fig. 2d). The background large-scale circulation for the catastrophic flood in the summer of 2003 has been discussed in the literature. For example, Zhang et al. (2004a) found that, in the summer of 2003, the Western Pacific Subtropical High (WPSH) was much stronger than normal with its location extending farther westward. This led to convergence between the southerly anomaly on the west flank of the WPSH and the north-easterly anomaly over the Huaihe River basin. Furthermore, a blocking situation over the mid-high latitudes and a strong upper-layer westerly jet promoted heavy rainfall in the Huaihe River basin. The stable and persistent WPSH also induced heat and drought over South China (Liu et al. 2006). However, no previous study has examined the possible impact of thermal forcing over the TP on the EASM in 2003.

3.2 Results of CTL03

It remains a great challenge for regional climate models to simulate the EASM, particularly its rainfall (Fu et al. 2005). Thus, it is necessary to demonstrate the WRF's performance in simulating the circulation and rainfall for the 2003 case before running the sensitivity experiment. In the upper troposphere, the South Asian High (SAH) is the major circulation system in the Northern Hemisphere in summer, and its formation and variation are closely related to diabatic heating over the TP (Zhu et al. 1981; Qian et al. 2002). In addition, the EASM rainfall belt usually occurs to the north of the low-level southwesterly jet and to the south of the upper westerly jet (Cressman 1981). The summer mean wind vector and westerly jet stream at 200 hPa in NCEP-FNL and the CTL03 run are shown in Fig. 3a and b, respectively. The CTL03 run reproduces well both the SAH and the westerly jet in the upper troposphere. It also captures the fields of the 850 hPa wind vector and surface air temperature (Fig. 3c, d), although the low-level southwesterly is somewhat stronger than in the NCEP-FNL data.

In the TRMM data (Fig. 4a), there is an obvious rainfall center over the Huaihe River valley in the summer of 2003, located between the upper westerly jet and the lower southwesterly jet. The CTL03 run captures the observed pattern of summer precipitation well in East China (Fig. 4b). The temporal evolution from June to August of

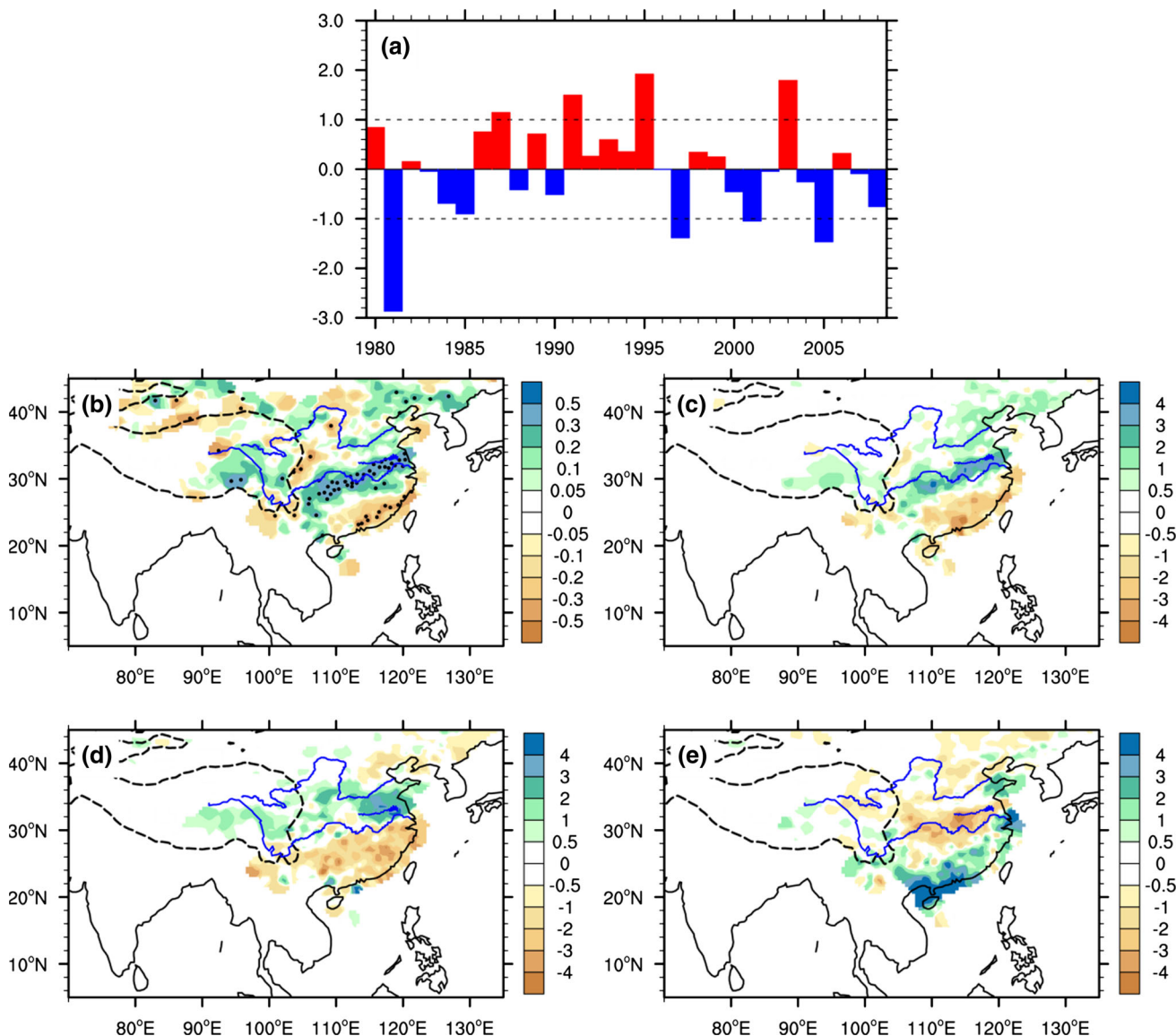


Fig. 2 **a** Time series of the standardized anomalies of the spring mean sensible heat (SH) averaged from the 73 stations over the TP with the linear trend excluded. **b** Spatial distribution of correlation coefficient between the 73-station-averaged spring SH index over the TP and summer (June–August) precipitation at 602 stations across China in 1980–2008 (the dotted regions are significant at the 90 % confidence level). The spring SH and precipitation are linearly detrended before the correlation is calculated. **c** Difference field at 602 stations in summer precipitation (mm day⁻¹) between the four

strongest spring SH years (1987, 1991, 1995, 2003) and the four weakest years (1981, 1997, 2001, 2005). **d** Precipitation anomaly (mm day⁻¹) in the summer of 2003 relative to the climatological mean (1980–2008). **e** As in **d**, but for the summer of 2001. The blue curves represent the Yangtze, Huaihe, and Huanghe rivers from south to north, and the dashed black curve denotes the area of the TP above 2000 m (rivers and terrain height are also shown in the following figures)

the domain-averaged precipitation over the Huaihe River basin in the CTL03 run agrees well with the station observations and TRMM data, in particular the torrential rain during the period from mid-June to July (Fig. 4c). Overall, the results from the CTL03 run demonstrate the capability of the WRF model in simulating both the circulation systems and rainfall pattern of the 2003 EASM. This provides us with the confidence to conduct the following sensitivity experiment.

4 Time-lagged effect of spring SH over the TP

4.1 Thermal forcing over the TP in summer

As introduced in Sect. 2, the difference between the CTL03 and ExpS03 runs reflects the contribution from the spring SH source over the TP. Can the spring SH anomaly over the TP persist until summer? To clarify this point, we show the difference field of summer SH between CTL03 and

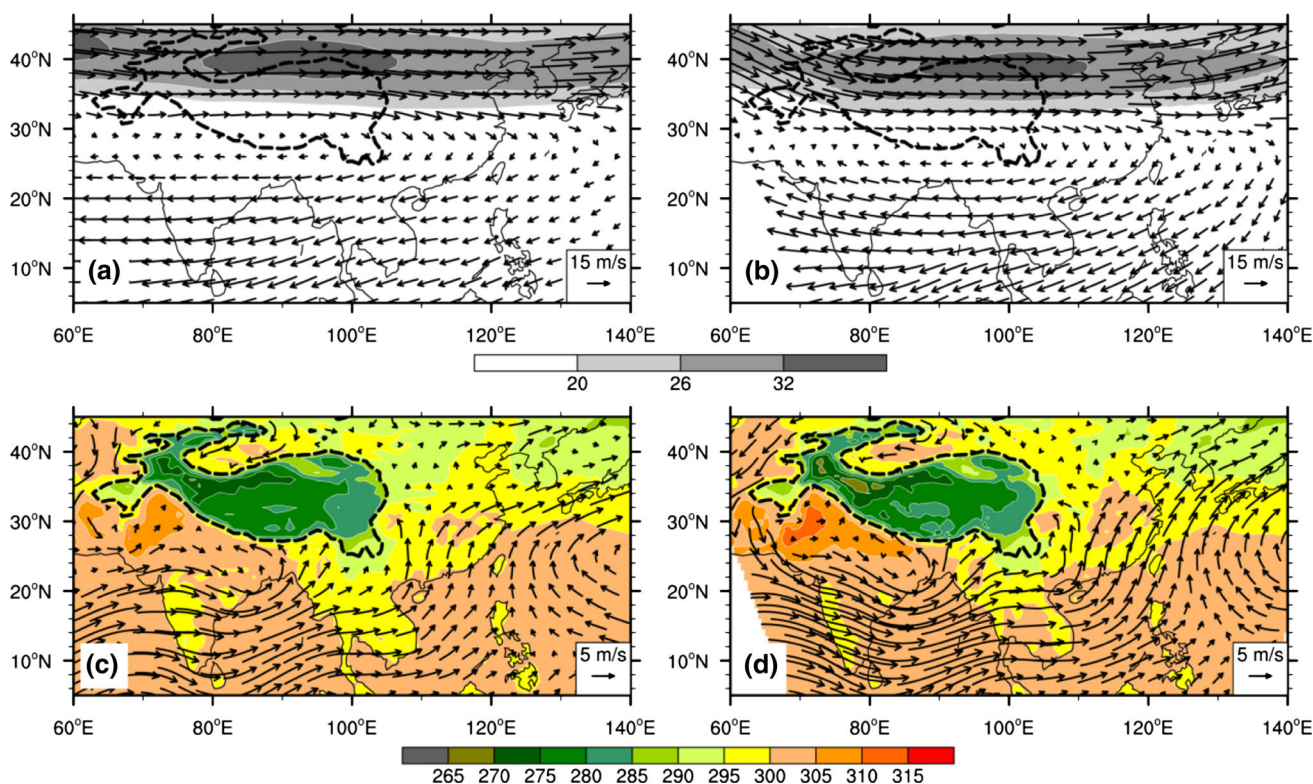


Fig. 3 Distribution of 200 hPa wind vectors (m s^{-1}) and the westerly jet (grey shading, m s^{-1}), defined by zonal wind speed above 20 m s^{-1} , in the summer of 2003 from **a** NCEP-FNL and **b** CTL03;

and 850 hPa wind vectors (m s^{-1}) and air temperature at 2 m above the surface (color shading, K) in the summer of 2003 from **c** NCEP-FNL and **d** CTL03

ExpS03 in Fig. 5a. A significant positive SH anomaly with a magnitude above 3 W m^{-2} remains over the northwestern TP after spring. Simultaneously, the obvious positive latent heat anomaly appears over the eastern TP in Fig. 5a. In the climate mean, the dominant surface heat flux over the northwestern TP in summer is SH, while latent heat dominates the atmospheric diabatic heating in the southeastern TP due to monsoon precipitation (e.g., Ye and Gao 1979; Duan and Wu 2005). The time series of the TP domain-averaged differences of daily SH and latent heat between the CTL03 and ExpS03 runs are shown in Fig. 5b. Note that the positive SH signal persists until the early August over the TP. The domain-averaged surface latent heat that is also presented, tends to be amplified.

More details of the thermal forcing over the TP in summer 2003 can be obtained by examining the vertical structure of the air temperature and diabatic heating differences between CTL03 and ExpS03. The difference in temperature over the TP region ($30\text{--}36^\circ\text{N}$) shows that the persistent summer SH in the western TP increases the air temperature efficiently above it, with the maximum temperature difference of $\sim 0.4 \text{ K}$ near the surface (Fig. 5c). The pressure-longitude cross-section of difference in atmospheric diabatic heating shown in Fig. 5d displays an eastward tilting in the vertical of the positive heating over

the western and mid TP, with the center appearing at about 500–350 hPa. Both the SH over the western TP and the latent heating to the east are intensified in summer due to the strong air-pumping effect of the spring SH. Significant positive diabatic heating also exists around the Huaihe River in East China centered at 250 hPa, consistent with the release of condensation latent heat due to the heavy rainfall.

According to thermal adaptation theory (Hoskins 1991; Wu and Liu 2000), the atmosphere responds to positive thermal forcing by forming a lower-layer cyclonic circulation and an upper-layer anticyclonic circulation. As required by the steady barotropic vorticity equation, airflows should converge at low levels and diverge at upper levels to the east of the diabatic heating area, with the reverse being true to the west (i.e., divergence at low levels and convergence at upper levels) (Duan and Wu 2005). Therefore, when a positive SH anomaly appears over the TP in spring, pumping processes arouse upward motion anomaly on its eastern side and downward motion anomaly on its western side. With the season evolution, the near-surface cyclonic anomaly and the upper-layer anticyclonic anomaly driven by the strong spring SH coincide with the climate mean surface warm low and the gigantic SAH above it in summer, and further reinforcing both of them.

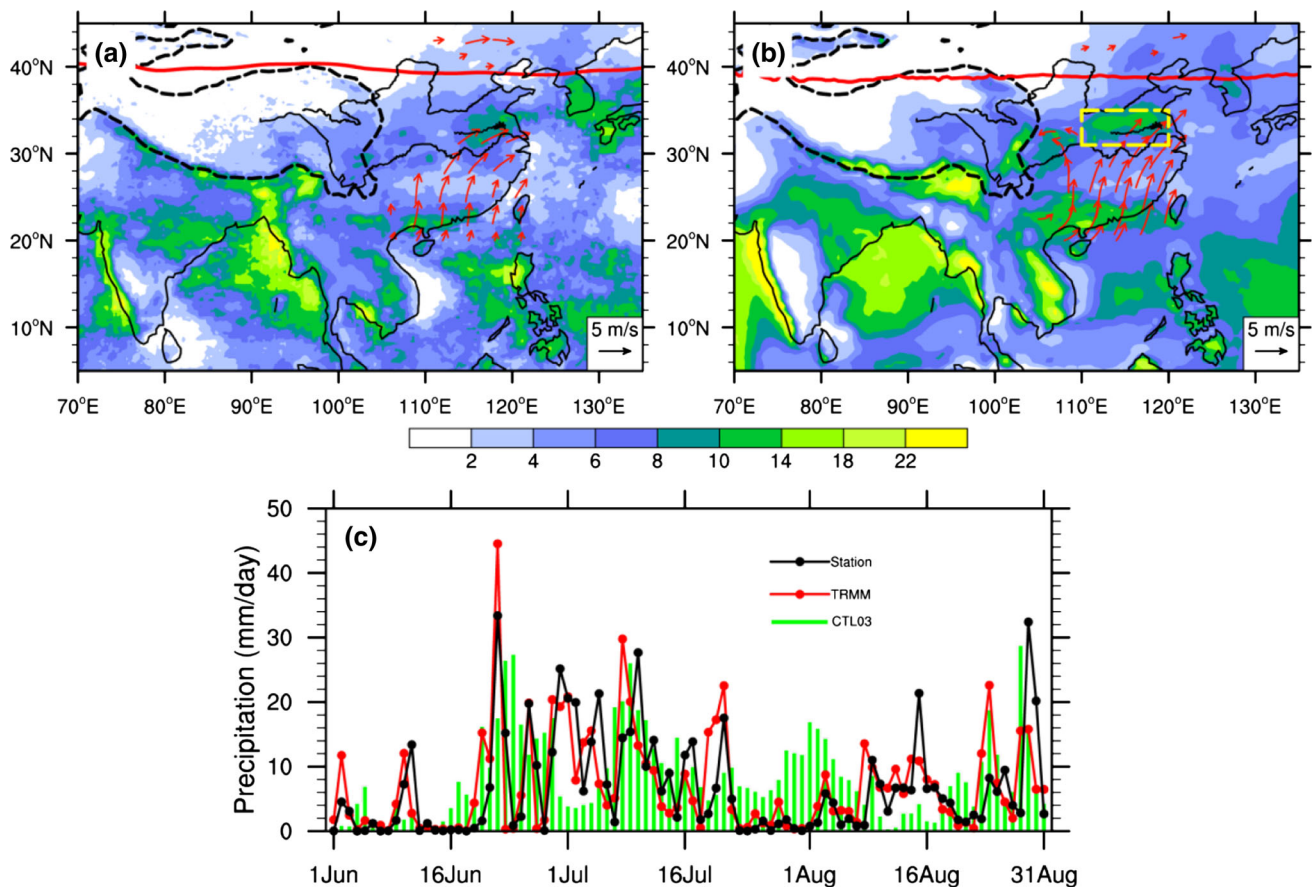


Fig. 4 Precipitation fields (color shading, mm day⁻¹) in summer 2003 from **a** the TRMM data and **b** the CTL03 run. The red solid curve represents the 200 hPa westerly jet axis, and the red vectors are the 850 hPa southwesterly jet (>2 m s⁻¹) over East China. **c** Time

series of the area averaged daily precipitation (mm day⁻¹) over the Huaihe River basin (31–35°N, 110–120°E, shown in **b**) from the station observations (black line), the TRMM data (red line), and the CTL03 run (bars)

Consequently, dry and cold northerlies tend to increase SH over the western TP, while wet and warm southerlies enhance latent heating over the eastern TP. Thus, in other words, a positive feedback process between diabatic heating and local atmospheric circulation appears over the TP, in which the “memory” of positive SH anomaly retains until summer by the enhanced dry and cold northerlies over the western TP (Fig. 5a). This assumption can be verified using the differences in summer circulation between CTL03 and ExpS03 (Fig. 6a–c). As a response to the positive diabatic heating over the western TP, an anomalous anticyclone is formed at 200 hPa, denoting the intensified SAH, while an anomalous cyclone around 85°E at 500 hPa enhances the surface warm low. Therefore, the positive feedback between diabatic heating and local circulation may contribute to the overall stronger summer atmospheric heat source over the TP.

Zhu et al. (2009) suggested that a weaker heat source over the TP could persist from spring until summer via long-term interactions between moist soil and the atmosphere. Recent studies also showed that the spring/summer

vegetation over the TP can notably impact the surface heating and Bowen ratio, and then change the circulation and precipitation over East China (Wang et al. 2009; Zuo et al. 2010). So, except for the positive feedback process between diabatic heating and local circulation, the characters of the land surface or soil may also contribute to the sustained spring SH.

4.2 Response of EASM to TP thermal forcing

Besides the local response of atmospheric circulations, the TP thermal forcing also exerts its impact on remote regions by generating standing waves (Hsu and Liu 2003; Liu et al. 2007; Chow et al. 2008). Following the procedure of Takaya and Nakamura (2001), the wave-activity fluxes are calculated to exhibit the wave energy transport. The disturbances due to the thermal forcing over the TP are always approximately stationary on a zonally varying basic flow. Under the westerly background, a significant wave-activity flux emanating from the TP propagates northeastward to North China and then southeastward into the northwestern

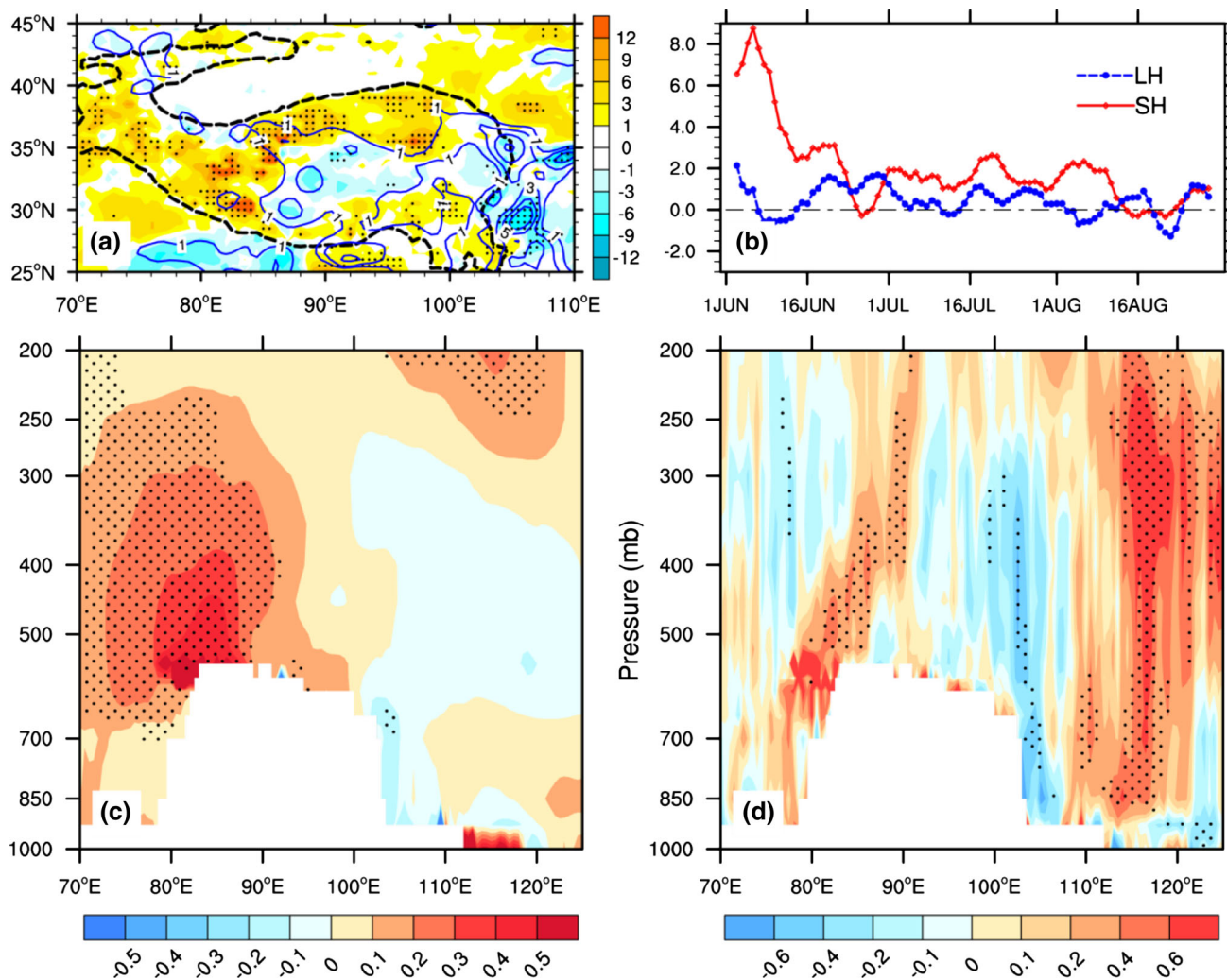


Fig. 5 **a** Difference fields of sensible heat (shading, $W m^{-2}$) and positive latent heat (Contours with the values larger than $1.0 W m^{-2}$) in the summer of 2003 between CTL03 and ExpS03 around the TP. **b** Time series of the TP domain-averaged differences in sensible heat (red) and latent heat (blue) between the CTL03 and ExpS03 runs ($W m^{-2}$). **c** Pressure–longitude cross-section of the air temperature

difference in the summer of 2003 between the CTL03 and ExpS03 runs (K) averaged from 30°N to 36°N. **d** As in **c**, but for atmospheric diabatic heating ($K day^{-1}$). The dots indicate the differences are statistically significant at the 90 % level for **a** sensible heat, **c** air temperature and **d** diabatic heating

Pacific (Fig. 6d). Circulation anomalies present a baroclinic vertical structure over the western and central TP (i.e., the anomalous heating regions) and an equivalent barotropic vertical structure in the areas away from the TP. A negative center of stream function is formed over northern China, corresponding to a cyclonic anomaly. Over the northwestern Pacific, however, an anticyclonic anomaly with a positive stream function is evident, which is consistent with the observed stronger and westward-extending WPSH in summer 2003, as documented by Zhang et al. (2004a). This spatial pattern and the two wave-like structures are consistent with the characteristics of Rossby waves forced by diabatic heating (Hoskins and Karoly 1981), suggesting that the positive anomaly in the atmospheric heat source over the TP generates a Rossby wave train to be downstream.

The cyclonic circulation response to the northeast TP generates a low-level northerly anomaly over northern China, while the anticyclonic circulation response over the subtropical western Pacific leads to a low-level southerly anomaly on its western flank. As a result, a cold and dry airflow from mid to high latitudes, and a warm and wet airflow converge over the Huaihe River basin. In particular, the low-level southerly anomaly conveys more water vapor to the Huaihe River basin, giving rise to a distinct moisture convergence belt (Fig. 7a). The precipitation difference field between the CTL03 and ExpS03 runs shows a clear positive value ($>2 mm day^{-1}$) in the Huaihe River basin (Fig. 7b), as expected from the circulation and moisture conditions. Thereby, the anomalous thermal forcing of the TP forces Rossby waves, which in turn affect the EASM

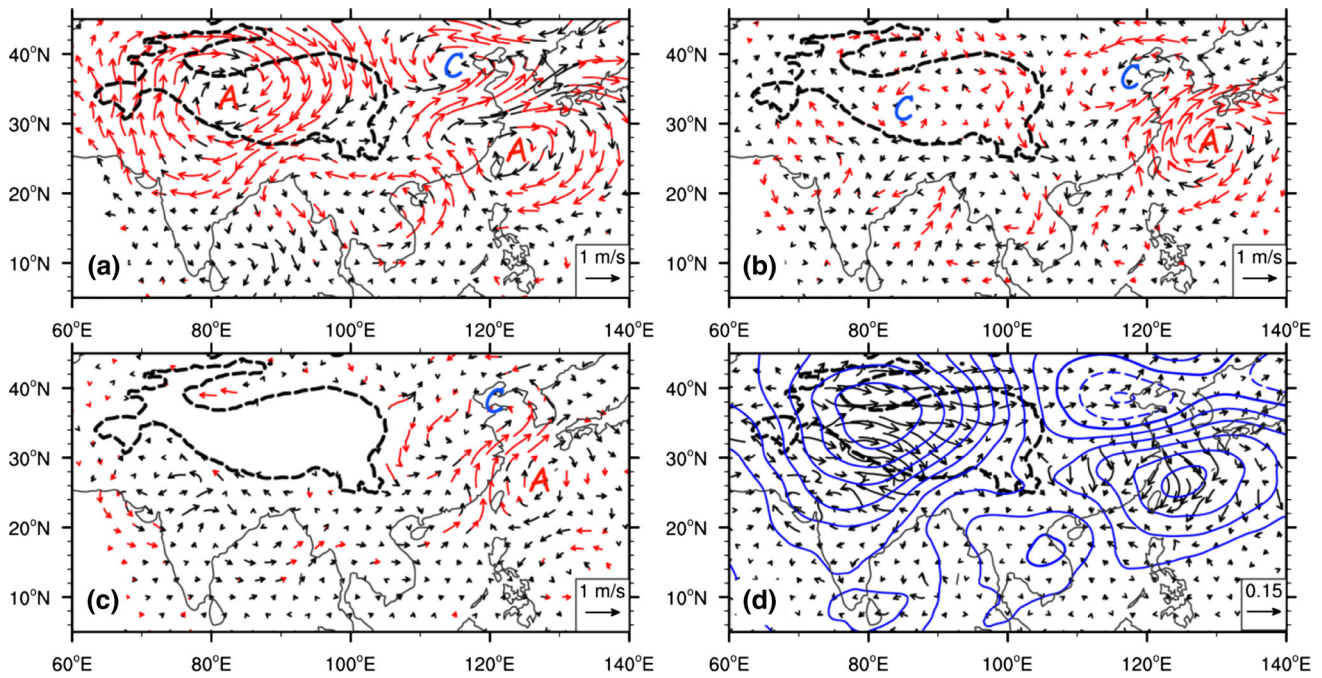


Fig. 6 Difference fields in wind vectors (m s^{-1}) in the summer of 2003 between the CTL03 and ExpS03 runs at **a** 200 hPa, **b** 500 hPa, and **c** 850 hPa; red vectors are significant at the 90 % confidence

level. **d** Difference field in the 200 hPa wave-activity flux (vectors, $\text{m}^2 \text{s}^{-2}$) and streamfunction (contours, interval is $2 \times 10^5 \text{ m}^2 \text{s}^{-1}$) in the summer of 2003 between the CTL03 and ExpS03 runs

circulation system. This conclusion is supported by the following facts. First, the diabatic heating over the TP is a persistent feature lasting from spring to summer, meaning

forcing of the TP, the thermodynamic equilibrium is diagnosed (Rodwell and Hoskins 2001). The thermodynamic energy equation in pressure coordinates is

$$\overline{\frac{\partial T}{\partial t}} = \underbrace{\frac{\overline{Q}}{C_p}}_A - \underbrace{\left(\frac{P}{P_0}\right)^{R/C_p} \overline{\omega} \frac{\partial \overline{\theta}}{\partial p}}_B - \underbrace{\overline{V} \cdot \nabla_p \overline{T}}_C - \underbrace{\left(\frac{P}{P_0}\right)^{R/C_p} \overline{\omega}' \frac{\partial \theta'}{\partial p}}_E - \underbrace{\overline{V}' \cdot \nabla_p T'}_F,$$

it is likely to be a forcing to the circulation rather than a response. Second, the spatial distribution of the vertical and horizontal structure exhibits forced Rossby wave characteristics.

The westerly flow in the mid and upper troposphere transports warm air over the TP to the downstream (Fig. 8a); this is an important driver of the Meiyu-Baiu rain band (Sampe and Xie 2010). As mentioned before, an obvious warm anomaly center exists over the western TP in summer, as seen in the difference between CTL03 and ExpS03 (Fig. 5c). The difference field of 500 hPa horizontal temperature advection between CTL03 and ExpS03 (Fig. 8b) indicates a positive difference in temperature advection above the Huaihe River basin, overlapping the anomalous strong upward motion.

To confirm the connection between the upward motion anomaly over the Huaihe River basin and the thermal

where the overbar denotes the time mean, primed quantities signify a deviation from the time mean, Q is diabatic heating, P_0 is standard constant pressure (1,000 hPa), and other notations are standard. When we consider the seasonal time scale, the temperature tendency term (A) is negligible, and the transient terms (E and F) are small in summer. The thermodynamic balance is attained mainly by the diabatic forcing term (B), the vertical temperature advection term (C), and the horizontal advection term (D). The differences in diabatic heating between CTL03 and ExpS03 are positive over the Huaihe River basin (Fig. 5d), and differences in horizontal temperature advection are also positive (Fig. 8b). Therefore, the changes in the B and D terms in the above equation have the same sign and must be balanced by a change in the vertical advection term (C). As a result, there will be stronger upward air motion ($\overline{\omega} < 0$) in the Huaihe River valley

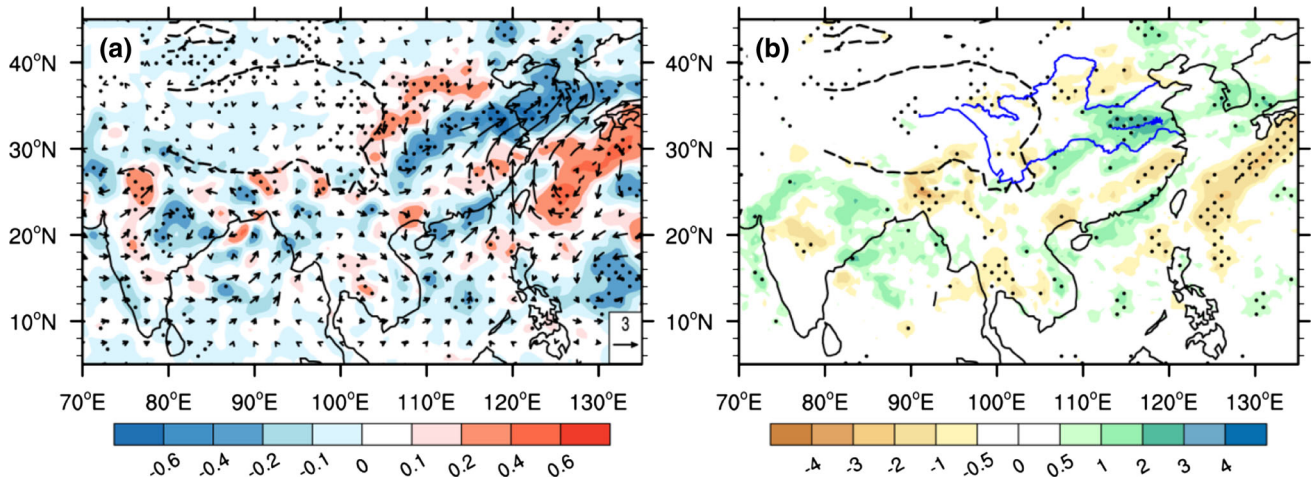


Fig. 7 Difference fields between the CTL03 and ExpS03 runs of **a** surface-300 hPa vertically integrated moisture divergence (shading, $10^{-5} \text{ kg m}^{-2} \text{ s}^{-1}$) and moisture transport (vectors, $10^{-5} \text{ kg m}^{-1} \text{ s}^{-1}$),

and **b** precipitation (mm day^{-1}) in the summer of 2003. The *dots* indicate the grids of difference fields for moisture divergence in Fig. 7a and precipitation in Fig. 7b are statistically significant at the 90 % level

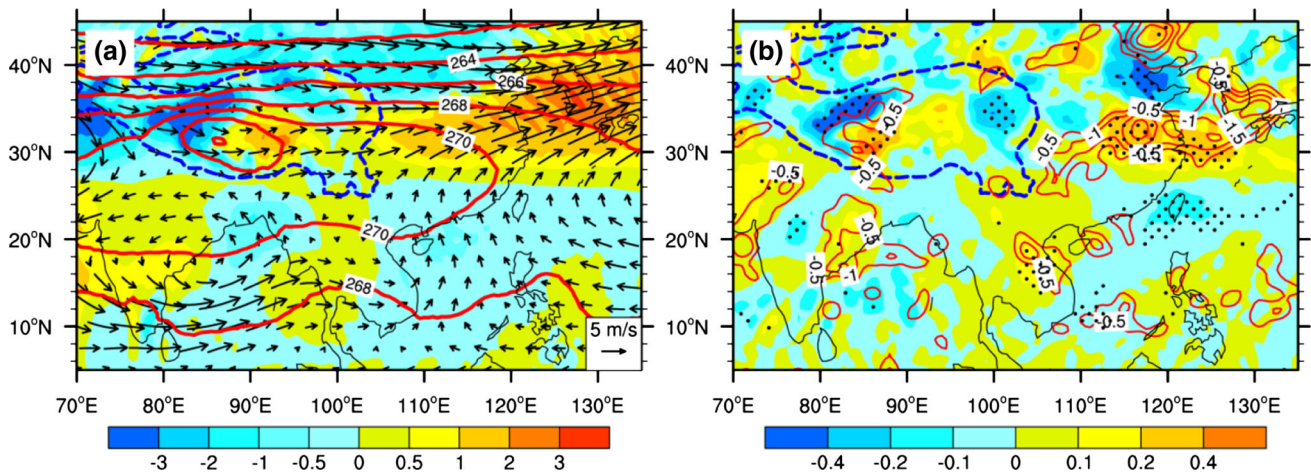


Fig. 8 a The 500 hPa wind vectors (m s^{-1}), air temperature (contours, K) and horizontal advection of temperature (shading, 10^{-5} K s^{-1}) in the summer of 2003 for the CTL03 run. **b** Difference fields of the 500 hPa horizontal advection of temperature (shading, 10^{-5} K s^{-1}) and negative ω (dP/dt , the values less than

$-0.5 \times 10^{-2} \text{ Pa s}^{-1}$ are shown with the red contours) in the summer of 2003 between the CTL03 and Exp03 runs; the dotted regions are significant at the 90 % confidence level for the advection of temperature

(since $\frac{\partial \theta}{\partial p}$ is negative). However, the diabatic heating strongly interacts with upward motion, and it is difficult to identify causality between them. Conversely, the horizontal temperature advection is independent of the local diabatic heating, as shown by Sampe and Xie (2010) with a linear baroclinic model, and it is produced by advecting warm air from the TP through the westerly jet stream. Therefore, the warm advection anomaly originating over the TP intensifies the upward motion substantially over the Huaihe River basin. Moreover, the condensation latent heat release due to precipitation further amplifies the ascending motion through a local diabatic enhancement (Rodwell and Hoskins 2001).

Torrential rainfall over East China often has the origin from the TP. In the summer of 2003, several meso- α scale upper-level troughs migrated from the TP and were embedded in the Meiyu-Baiu front, making a considerable contribution to the flooding over the Huaihe River basin (Zhang et al. 2004a). Figure 9a shows the temporal-zonal cross-section of vorticity difference at 500 hPa averaged over the band 30–36°N, which covers the latitudes of the Yangtze and Huaihe River basins. Frequent positive vorticity anomalies are generated to the west of 90°E due to the strong SH forcing, and some of them even propagate eastward to East China. These eastward-propagating synoptic disturbances might be important triggers for the

torrential rainfall in the Huaihe River basin. Comparing Fig. 9a with Fig. 4c, several torrential rain processes during the period from mid-June to July over the Huaihe River basin occur when positive vorticity develops over the TP and propagates eastward, implying a synoptic impact of the TP on the downstream rainfall anomaly. This conclusion can be verified by the precipitation probability density function (PDF) in the CTL03 and ExpS03 runs (Fig. 9b). Both the total and extreme rainfall amount are obviously larger in the CTL03 run than in ExpS03, and no torrential rainfall events above 82 mm day^{-1} occur in ExpS03. It is likely that, in addition to regulating the large-scale circulation by generating steady waves, the synoptic impact of the TP thermal forcing might be more important for the summer flood in the Huaihe basin in 2003.

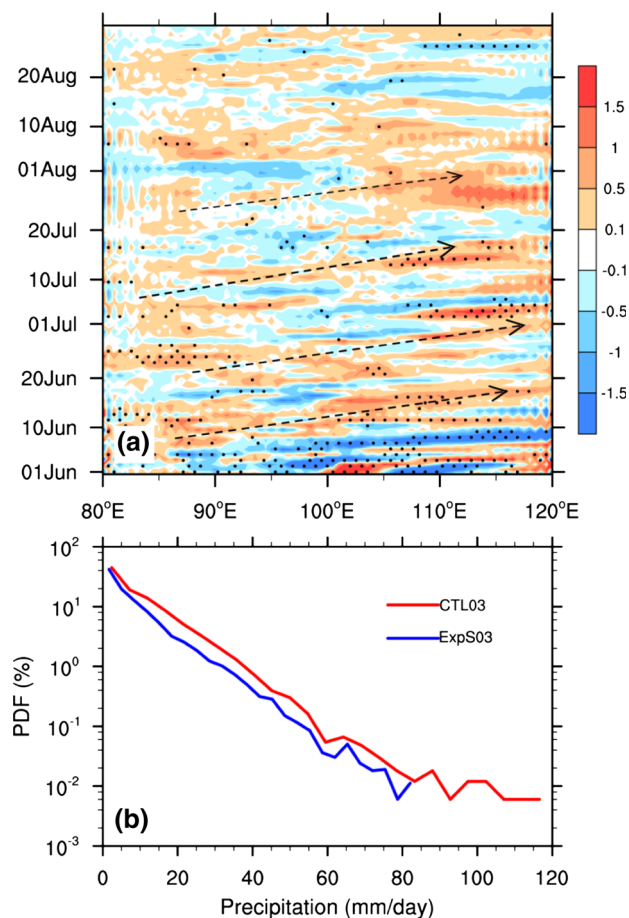


Fig. 9 **a** Temporal-zonal cross-section of 500 hPa vorticity (10^{-5} s^{-1}) difference between the CTL03 and ExpS03 runs averaged from 30°N to 36°N ; the dotted regions are significant at the 90 % confidence level. **b** Probability distribution function (PDF) of daily precipitation over the Huaihe River basin ($31\text{--}35^{\circ}\text{N}$, $110\text{--}120^{\circ}\text{E}$) in the summer of 2003 for the CTL03 (red) and ExpS03 (blue) runs

4.3 2001 case study

To verify the robustness of the conclusions obtained from the 2003 case study, similar numerical experiments were performed for 2001, a year with a negative spring SH anomaly over the TP and typical drought in the Yangtze and Huaihe River basins in summer (Fig. 2e). The weak SH over the TP reduces the lower southerly and the relevant moisture transport over East China, with moisture divergence and less rainfall occurring in the Yangtze and Huaihe River basins (Fig. 10a, b). Owing to the lowered heating, the warm center over the TP is also reduced substantially (Fig. 10c) and results in a cold advection anomaly and suppresses upward motion over the downstream regions including the Yangtze and Huaihe River basins (Fig. 10d). Furthermore, the eastward-travelling synoptic systems originating from the TP are decreased due to the weakened thermal forcing over the TP (figure not shown). This case study provides further evidence of the important role of the spring SH anomaly over the TP in regulating the variability of EASM and the rainfall anomaly over East China.

5 Summary and discussion

This study used the WRF regional model to assess the time-lagged impact of the spring SH source over the TP on the summer rainfall anomaly in East China. A typical positive spring SH anomaly over the TP and a strong EASM occur in 2003 with precipitation substantially above normal and flooding over the Huaihe River basin. Numerical simulations indicate that strong spring SH over the TP can persist until summer and lead to an overall strong atmospheric heat source in the subsequent summer, characterized by increased SH over the western TP and increased latent heating to the east. The heating intensifies the local surface warm low and the SAH, and also forces a Rossby wave train in the downstream region. The cyclone generated to the northeast of the TP gives a low-level northerly anomaly over northern China, while the anticyclone generated over the western Pacific enhances the WPSH and the resultant low-level southerly on its western flank over South China. As a result, a convergence zone appears over the Huaihe River valley. In addition, the persistent positive SH enhances the warm center over the TP, resulting in anomalous eastward warm advection and vigorous upward motion over the convergence zone. Favorable circulation conditions and abundant moisture transport due to the anomalous lower southerly, together with the synoptic disturbances initiated over the TP, induce excessive precipitation and flooding over the Huaihe River basin.

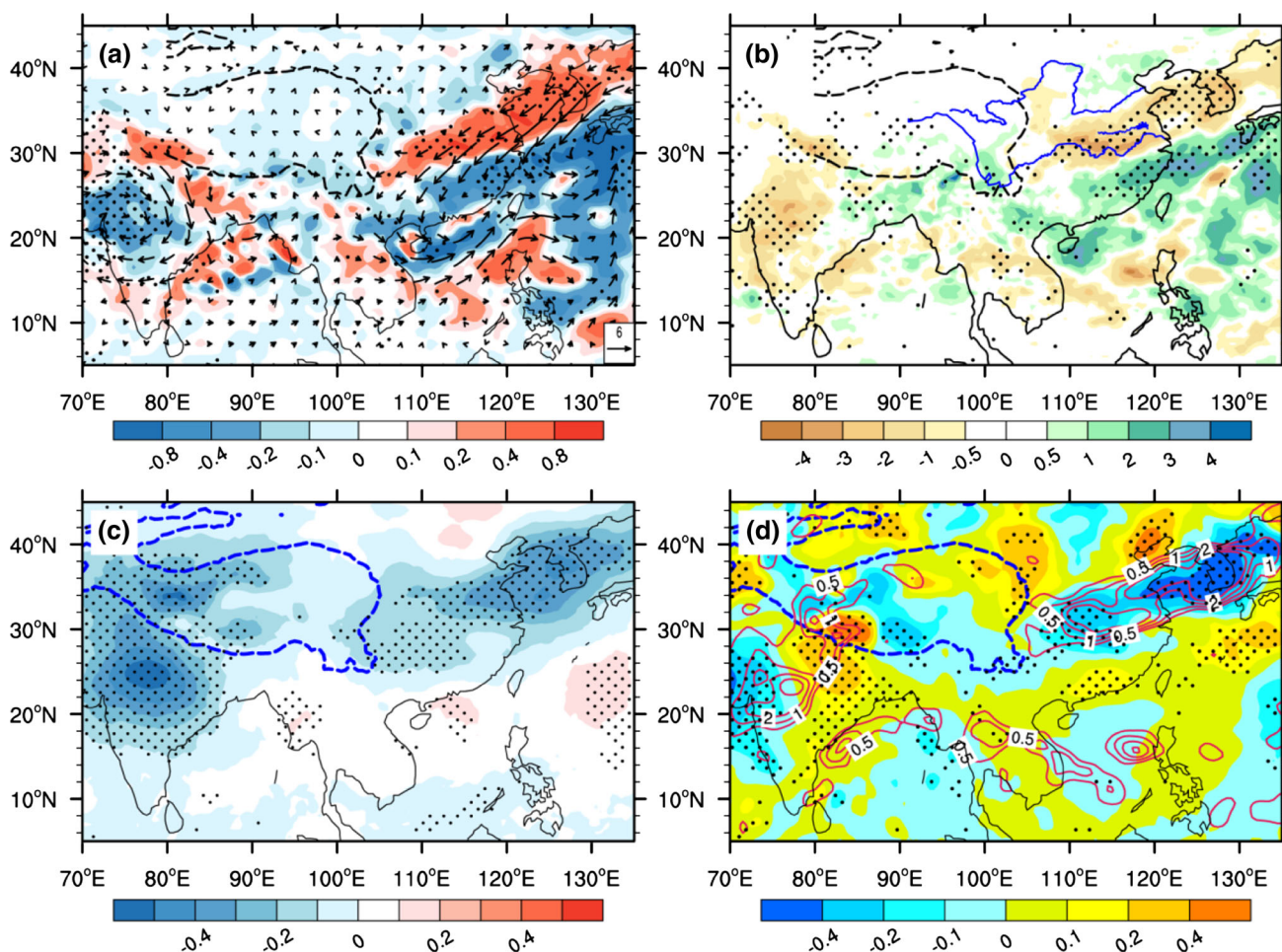


Fig. 10 Difference fields in the summer of 2001 between the CTL01 and ExpS01 runs for **a** surface-300 hPa vertically integrated moisture divergence (shading, $10^{-5} \text{ kg m}^{-2} \text{ s}^{-1}$) and moisture transport (vectors, $10^{-5} \text{ kg m}^{-1} \text{ s}^{-1}$), **b** precipitation (mm day^{-1}), **c** 500 hPa air temperature (K), and **d** 500 hPa horizontal advection of

temperature (shading, 10^{-5} K s^{-1}) and positive ω (DP/dt , the values larger than $0.5 \times 10^{-2} \text{ Pa s}^{-1}$ are shown with the red contours). The dotted regions are significant at the 90 % confidence level for **a** moisture divergence, **b** precipitation, **c** air temperature and **d** temperature advection

The reverse situation in 2001, with weak spring SH over the TP and a southward retreating summer rainfall belt in East China, has also been investigated. Simulation results provide further evidence to demonstrate the important role of the thermal forcing over the TP on the EASM anomaly. Therefore, in addition to regulating the timing of EASM onset, the spring SH anomaly over the TP influences the interannual variability of EASM in terms of wave activity and synoptic disturbance.

The EASM is impacted by the superposition of many factors covering a wide range of spatial and temporal scales (Ding and Chan 2005; Wang 2006). For example, there is a remarkable negative SH anomaly in the spring of 2005 over the TP (Fig. 2a), while excessive precipitation also occurred in the Huaihe River basin during the subsequent summer (figure not shown). Hence, there must be other factors responsible for the rainfall anomalies over East China in this year. To identify the intrinsic connection

among the various factors regulating the EASM, we need to study more examples to exclude the dependence on individual conditions.

Moreover, as reviewed in Sect. 1, there is a positive correlation between the summer rainfall in the Yangtze and Huaihe River basins, and winter-spring snow cover/depth or spring SH over the TP. However, snow cover/depth may restrain the upward SH and latent heat flux due to the increased albedo and decreased surface temperature (Chen et al. 2000; Zhang and Tao 2001). Thus, a question emerges, that is, why above-normal winter snow cover/depth correspond to strong in situ spring SH. This issue will be investigated in our future work.

Acknowledgments We thank Dr. Schneider and two anonymous reviewers for their constructive comments; and also thank Meirong Wang for helpful discussions. This work was supported jointly by the Chinese Ministry of Science and Technology (grant 2010CB951703; 2012CB417203), the Chinese Ministry of Finance/Ministry of Science

and Technology (GYHY201006014), and the National Natural Science Foundation of China (grant 41175070; 41275088; 41275095).

References

- Ai X (2002) General circulation over the northern hemisphere in 2001 and its impact on the climate in China. *Meteor Mon* 28(4):21–24 (in Chinese)
- Bougeault P, Lacarrère P (1989) Parameterization of orographic induced turbulence in a mesobeta scale model. *Mon Weather Rev* 117:1872–1890
- Chen F, Dudhia J (2001) Coupling an advanced land-surface hydrology model with the Penn Statr-NCAR MM5 modeling system. Part I: model implementation and sensitivity. *Mon Weather Rev* 129:569–585
- Chen QJ, Gao B, Zhang Q (2000) Studies on Relation of snow cover over the Tibetan Plateau in winter-summer monsoon change. *Chin J Atmos Sci* 24(4):477–492 (in Chinese)
- Chou MD, Suarez MJ (1999) A shortwave radiation parameterization for atmospheric studies. NASA Tech Memo 15(104606), 40 pp
- Chow KC, Chan JCL, Shi XL, Liu YM, Ding YH (2008) Time-lagged effects of spring Tibetan Plateau soil moisture on the monsoon over China in early summer. *Int J Climatol* 28:55–67
- Cressman GP (1981) Circulation of the West-Pacific jet stream. *Mon Weather Rev* 109:2450–2463
- Ding YH, Chan JCL (2005) The East Asian summer monsoon: an overview. *Meteorol Atmos Phys* 89:117–142. doi:10.1007/s00703-005-0125-z
- Duan AM, Wu GX (2005) Role of the Tibetan Plateau thermal forcing in the summer climate pattern over subtropical Asia. *Clim Dyn* 24:793–807
- Duan AM, Liu YM, Wu GX (2005) Heating status of the Tibetan Plateau from April to June and rainfall and atmospheric circulation anomaly over East Asia in midsummer. *Sci China Ser D* 48:250–257
- Duan AM, Li F, Wang MR, Wu GX (2011) Persistent weakening trend in the spring sensible heat source over the Tibetan Plateau and its impact on the Asian summer monsoon. *J Clim* 24:5671–5682
- Duan AM, Wang MR, Lei YH, Cui YF (2012) Trends in summer rainfall over China associated with the Tibetan Plateau sensible heat source during 1980–2008. *J Clim* 25:261–274. doi:10.1175/JCLI-D-11-00669.1
- Fu CB, Teng XL (1988) Relationship between summer climate in China and El Nino/Southern Oscillation phenomenon. *Chin J Atmos Sci* 12:133–141 (in Chinese)
- Fu C, Wang S, Xiong Z, William JG, Lee DK, McGergor JL, Sato Y, Kato H, Kim JW, Suh MS (2005) Regional climate model intercomparison project for Asia. *Bull Amer Meteor Soc* 86:257–266
- Gao R, Zhong HL, Dong WJ, Wei ZG (2011) Impact of snow cover and frozen soil in the Tibetan Plateau on summer precipitation in China. *J Glaciol Geocryol* 33:254–260 (in Chinese)
- Grell G, Devenyi D (2002) A generalized approach to parameterizing convection combining ensemble and data assimilation techniques. *Geophys Res Lett* 29(14):31–38
- Hoskins B (1991) Toward a PV- θ view of the general circulation. *Tellus* 43AB:27–35
- Hoskins B, Karoly D (1981) The steady linear response of a spherical atmosphere to thermal and orographic forcing. *J Atmos Sci* 38(1179–1196):258
- Hsu HH, Liu X (2003) Relationship between the Tibetan Plateau heating and East Asian summer monsoon rainfall. *Geophys Res Lett* 30(20):2066. doi:10.1029/2003GL017909
- Huffman GJ, Adler RH, Bolvin DT, Gu GJ, Nelkin EJ, Bowman KP, Hong Y, Stocker EF, Wolff DB (2007) The TRMM multi-satellite precipitation analysis: quasi-global, multi-year, combined-sensor precipitation estimates at fine scale. *J Hydrometeorol* 8:38–55
- Kim EJ, Hong SY (2010) Impact of air-sea interaction on East Asian summer monsoon climate in WRF. *J Geophys Res* 115:D19118. doi:10.1029/2009JD013253
- Kim HJ, Wang B (2011) Sensitivity of the WRF model simulation of the East Asian summer monsoon in 1993 to shortwave radiation scheme and ozone absorption. *Asia-Pacific J Atmos Sci* 47(2):167–180
- Li GP, Zhao BJ, Yang JQ (2002) A dynamical study of the role of surface sensible heating in the structure and intensification of the Tibetan Plateau vortices. *Chin J Atmos Sci* 26(4):519–525 (in Chinese)
- Lin YL, Farley RD, Orville HD (1983) Bulk parameterization of the snow field in a cloud model. *J Clim Appl Meteorol* 22:1065–1092
- Liu HZ, Zhao SR, Zhao CG, Lu ZS (2006) Weather abnormal and evolutions of Western Pacific Subtropical High and South Asian High in summer of 2003. *Plateau Meteorol* 25(2):169–178 (in Chinese)
- Liu YM, Hoskins BJ, Blackburn M (2007) Impact of Tibetan Orography and Heating on the Summer Flow over Asia. *J Met Soc Japan* 85B:1–19
- Liu YM, Wu GX, Hong JL, Dong BW, Duan AM, Bao Q, Zhou LJ (2012) Revisiting Asian monsoon formation and changes associated with Tibetan Plateau forcing: II. Change. *Clim Dyn*. doi:10.1007/s00382-012-1335-y
- Luo HB, Chen R (1995) The impact of the anomalous heat sources over the eastern Tibetan Plateau on the circulation over the East Asia in summer half year. *Acta Meteor Sinica* 15(4):94–102 (in Chinese)
- Luo HB, Yanai M (1983) The larger-scale circulation and heat sources over Tibetan Plateau and surrounding areas during early summer of 1979, Part I: precipitation and kinetic analysis. *Mon Weather Rev* 111:922–944
- Luo HB, Yanai M (1984) The large-scale circulation and heat sources over the Tibetan Plateau and surrounding areas during the early summer of 1979. Part II: heat and moisture budgets. *Mon Weather Rev* 112:966–989
- Mlawer EJ, Taubman SJ, Brown PD, Iacono MJ, Clough SA (1997) Radiative transfer for inhomogeneous atmospheres: RRTM a validated correlated-k model for the long wave. *J Geophys Res* 102:16663–16682. doi:10.1029/97JD00237
- Qian YF, Zhang Q, Yao YH, Zhang XH (2002) Seasonal variation and heat preference of the South Asia high. *Adv Atmos Sci* 19(5):821–836
- Qian YF, Zheng YQ, Zhang Y, Miao MQ (2003) Responses of China's summer monsoon climate to snow anomaly over the Tibetan Plateau. *Int J Climatol* 23:593–613
- Qin D, Liu S, Li P (2006) Snow cover distribution, variability, and response to climate change in western China. *J Clim* 19:1820–1833
- Reynolds RW, Smith TM, Liu C, Chelton DB, Casey KS, Schlax MG (2007) Daily high-resolution-blended analyses for sea surface temperature. *J Clim* 20:5473–5496
- Rodwell MJ, Hoskins BJ (2001) Subtropical anticyclones and summer monsoons. *J Clim* 14:3192–3211
- Sampe T, Xie SP (2010) Large-scale dynamics of the Meiyu-Baiu rainband: environmental forcing by the westerly jet. *J Clim* 23:113–134
- Takaya K, Nakamura H (2001) A formulation of a phase-independent wave-activity flux for stationary and migratory quasigeostrophic eddies on a zonally varying basic flow. *J Atmos Sci* 58:608–627

- Tao SY, Ding YH (1981) Observational evidence of the influence of the Qinghai-Xizang (Tibet) Plateau on the occurrence of heavy rain and severe convective storms in China. *Bull Amer Meteor Soc* 62:23–30
- Wang B (1987) The development mechanism for Tibetan Plateau warm vortices. *J Atmos Sci* 44(20):2978–2994
- Wang B (2006) *The Asian monsoon*. Springer/Praxis Publishing Co., New York
- Wang B, Wu R, Fu X (2000) Pacific-East Asian teleconnection: How does ENSO affect East Asian climate? *J Clim* 13:1517–1536
- Wang B, Bao Q, Hoskins B, Wu G, Liu Y (2008) Tibetan Plateau warming and precipitation changes in East Asia. *Geophys Res Lett* 35:L14702. doi:10.1029/2008GL034330
- Wang YX, Zhao P, Yu RC, Rasul G (2009) Inter-decadal variability of Tibetan spring vegetation and its associations with eastern China spring rainfall. *Int J Climatol* 30:856–865
- Wu RG, Kirtman BP (2007) Observed relationship of spring and summer East Asian rainfall with winter and spring Eurasian snow. *J Clim* 20:1285–1304. doi:10.1175/JCLI4068.1
- Wu GX, Liu YM (2000) Thermal adaptation, overshooting, dispersion, and subtropical high Part I: thermal adaptation and overshooting. *Chin J Atmos Sci* 24(4):433–436 (in Chinese)
- Wu TW, Qian ZA (2003) The relationship between the Tibetan winter snow and the Asian summer monsoon and rainfall: an observational investigation. *J Clim* 16:2038–2051
- Wu GX, Li WP, Guo H (1997) Sensible heat driven air-pump over the Tibetan-Plateau and its impacts on the Asian Summer Monsoon. In: Ye DZ (ed) *Collections on the Memory of Zhao Jiuzhang*. Science Press, Beijing, pp 116–126
- Wu ZW, Wang B, Li JP, Jin FF (2009) An empirical seasonal prediction model of the East Asian summer monsoon using ENSO and NAO. *J Geophys Res* 114:D18120. doi:10.1029/2009JD011733
- Wu GX, Liu YM, He B, Bao Q, Duan AM, Jin FF (2012) Thermal controls on the Asian summer monsoon. *Sci Rep* 2:404
- Yanai M, Wu GX (2006) Effects of the Tibetan Plateau. In: Wang B (ed) *The Asian Monsoon*. Springer, New York, pp 513–549. doi:10.1007/3-540-37722-0_13
- Yang YW, Xu L, Gong ZS (2004) General circulation over the northern hemisphere in 2003 and its impact on the climate in China. *Meteor Mon* 30(4):20–24 (in Chinese)
- Yang HW, Wang B, Wang B (2011) Reduction of systematic biases in regional climate downscaling through ensemble forcing. *Clim Dyn*. doi:10.1007/s00382-011-1006-4
- Yasunari T, Miwa T (2006) Convective cloud systems over the Tibetan Plateau and their impact on Meso-scale disturbance in the Meiyu/Baiu frontal zone. *J Meteor Soc Japan* 84(4):783–803
- Ye DZ, Gao YX (1979) *Meteorology of the Qinghai-Xizang (Tibet) Plateau*. Science Press, Beijing (in Chinese)
- Zhang SL, Tao SY (2001) Influences of snow cover the Tibetan Plateau on Asian summer monsoon. *Chin J Atmos Sci* 25(3):372–390 (in Chinese)
- Zhang QY, Wang HJ, Lin ZH, Sun JH, Zhang XL, Wei J (2004a) The research of the reason for weather and climate anomaly in China: the year of 2003. China Meteorological Press, Beijing (in Chinese)
- Zhang YS, Li T, Wang B (2004b) Decadal change of the spring snow depth over the Tibetan Plateau: the associated circulation and influence on the East Asian summer monsoon. *J Clim* 17:2780–2793
- Zhao P, Chen LX (2001) Climate features of atmospheric heat source/sink over the Qinghai-Xizang Plateau in 35 years and its relation to rainfall in China. *Sci China Ser D* 44:858–864
- Zhao P, Zhou ZJ, Liu JP (2007) Variability of Tibetan spring snow and its associations with the hemispheric extratropical circulation and East Asian summer monsoon rainfall: an observational investigation. *J Clim* 20:3942–3955
- Zhu FK, Lu LH, Chen XJ (1981) *The South Asian High*. Science Press, Beijing, pp 1–94 (in Chinese)
- Zhu YX, Ding YH, Liu HW (2009) Simulation of the influence of winter snow depth over the Tibetan Plateau on summer rainfall in China. *Chin J Atmos Sci* 33:903–915 (in Chinese)
- Zuo ZY, Zhang RH, Zhao P (2010) The relation of vegetation over the Tibetan Plateau to the rainfall in China in boreal summer. *Clim Dyn*. doi:10.1007/s00382-010-0863-6